

Gas-phase formation of cationic fullerene/9-aminoanthracene clusters: an indicator for interstellar dust growth

Xiaoyi Hu,^{1,2,3} Deping Zhang,³ Congcong Zhang,⁴ Yuanyuan Yang,^{1,2,3} Yang Chen,³ Junfeng Zhen^{1,2,4}★ and Liping Qin^{1,2}

¹CAS Key Laboratory of Crust-Mantle Materials and Environment, University of Science and Technology of China, 96 Jinzhai Rd, Hefei, Anhui 230026, China

²CAS Center for Excellence in Comparative Planetology, 96 Jinzhai Rd, Hefei, Anhui 230026, China

³CAS Center for Excellence in Quantum Information and Quantum Physics, Hefei National Laboratory for Physical Sciences at the Microscale, Department of Chemical Physics, University of Science and Technology of China, 96 Jinzhai Rd, Hefei, Anhui 230026, China

⁴CAS Key Laboratory for Research in Galaxies and Cosmology, Department of Astronomy, University of Science and Technology of China, 96 Jinzhai Rd, Hefei, Anhui 230026, China

Accepted 2021 September 24. Received 2021 September 24; in original form 2021 June 2

ABSTRACT

Growth of clusters by adduction of monomers – as the first step in dust particle growth – is an area of much interest in astronomy. We focus on the fullerene/9-aminoanthracene cluster species, to illustrate the competition between the van der Waals bonding growth and the covalent bonding growth model versus the charge transfer model in the large cluster formation process. The experimental results show that fullerene-fragment (C_{56} and C_{58})/9-aminoanthracene cluster cations, e.g. $[(C_{14}H_{11}N)_n C_{56}]^+$ and $[(C_{14}H_{11}N)_n C_{58}]^+$, $n = [1, 7]$, are efficiently formed, while C_{60}^+ is insensitive to the cluster's formation. With laser irradiation, all the fullerene/9-aminoanthracene clusters dissociate into 9-aminoanthracene and fullerene cations. The mechanisms for the reactions of fullerene cations and 9-aminoanthracene were investigated by theoretical calculations, under the assumption that the molecular geometries found for the formed complexes correspond to the global energy minima: the absence of C_{60}^+ clusters is mainly due to the charge transfer channel's competition; $[(C_{14}H_{11}N)C_{58}]^+$ has three types of isomers, with van der Waals or covalent bonds, mainly depending on the reaction sites of fullerene cations. Importantly, in the size grown process, for the fullerene/9-aminoanthracene cluster there exists a geometry configuration conversion between the van der Waals and covalent bonding modes. The largest fullerene/9-aminoanthracene clusters, e.g. $[(C_{14}H_{11}N)_7 C_{58}]^+$ (240 atoms, ~ 4 nm in size), are likely in a multishelled geometry, i.e. seven 9-aminoanthracene molecules surrounding fullerene cations in two layers, which can directly build the relationship between molecular clusters and carbonaceous grains. Nitrogen matters! The specific side chains (e.g. $-NH_2$) play an important role in the growth of interstellar dust.

Key words: astrochemistry – molecular processes – methods: laboratory – ISM: molecules – ultraviolet: ISM.

1 INTRODUCTION

Studying the large molecules and interstellar dust grains that exist in space, especially in the range of ~ 100 – 200 atoms or nanometre sized, is a very interesting topic (Tielens 2013; Candian, Zhen & Tielens 2018 and references therein). The presence of large molecules may help to explain certain characteristics of astronomically observed IR spectra (Tielens 2008 and references therein). The origin and evolution of such large molecules and further interstellar nanometre-sized dust grains are not entirely clear in laboratory experiments; thus it is difficult to assess their formation and growth models in the interstellar medium (ISM) (Candian et al. 2018; Zhen, Chen & Tielens 2018; Martínez et al. 2020).

In the ISM, buckminsterfullerenes (C_{60}) have been confirmed to exist in many objects with the aid of mid-IR spectral observation

(Cami et al. 2010). Gas-phase laboratory spectral studies have also revealed C_{60}^+ as the carrier of several diffuse interstellar bands (Campbell et al. 2015; Walker et al. 2015; Cordiner et al. 2019). Based on the IR observations of interstellar reflection nebulae and laboratory experimental results, Berné & Tielens (2012) and Zhen et al. (2014) proposed that polycyclic aromatic hydrocarbons (PAHs) can convert into graphenes and subsequently to fullerenes (e.g. C_{60}). PAHs are abundant in many ISM objects, and PAHs are thought to form in the stellar ejecta; different sizes of PAHs either act as molecular building blocks or intermediate in the soot condensation process (Tielens 2008 and references therein). In the harsh environment of the ISM, these PAHs are further processed for some hundred million years (Sellgren 1984; Allamandola, Tielens & Barker 1989). As part of their evolution, PAHs may acquire functional groups, such as amino ($-NH_2$), methyl ($-CH_3$), methoxy ($-OCH_3$), alcohol ($-OH$), ketone ($>C=O$), cyano/isocyno ($-CN/NC$), and acid ($-COOH$) groups (Bernard-Salas et al. 2012).

★ E-mail: jfzhen@ustc.edu.cn

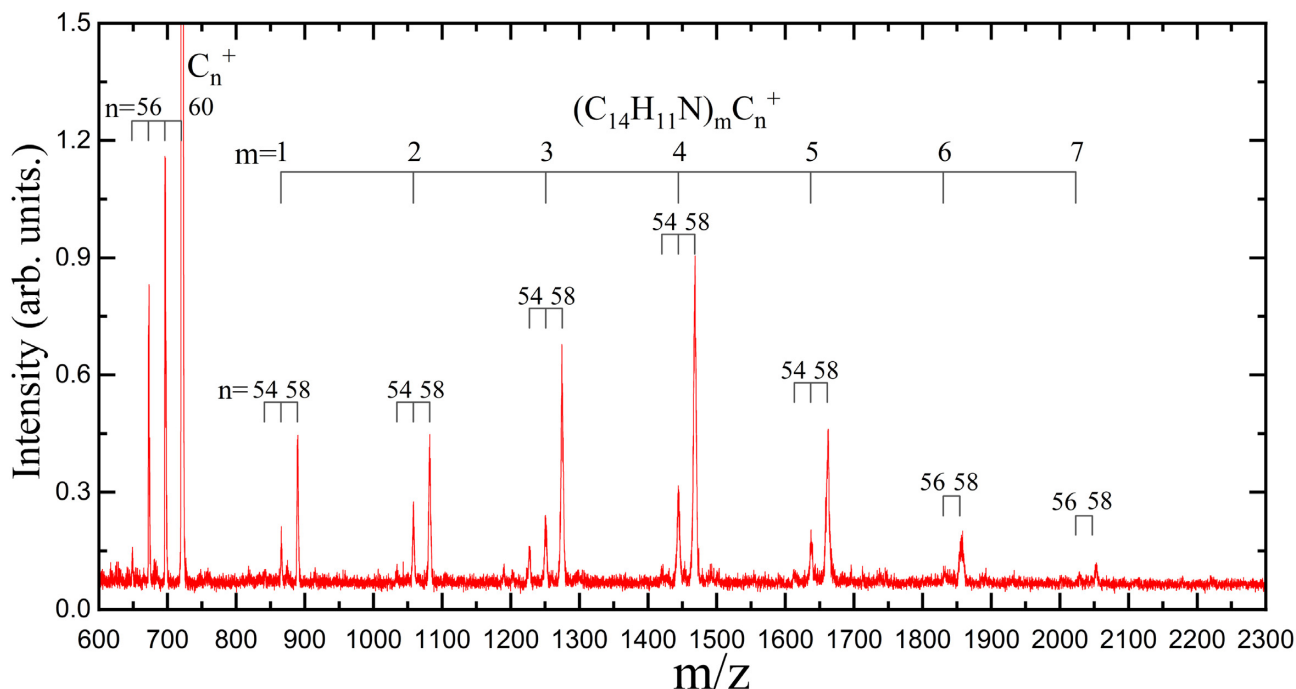


Figure 1. Mass spectrum of fullerene/9-aminoanthracene cluster cations recorded without laser irradiation: fullerene cations ($C_{60/58/56/54}^+$) and the newly formed fullerene/9-aminoanthracene cluster cations; $(C_{14}H_{11}N)_n C_{58/56}^+$ with $n = [1, 7]$ and $(C_{14}H_{11}N)_m C_{54}^+$ with $m = [1, 5]$ are labelled.

Fullerene readily reacts with other molecules, e.g. PAHs and their derivatives (Bohme 2016 and references therein). In the interstellar region where fullerenes and PAHs coexist, fullerene/PAH clusters and their associated derivate clusters may be formed through ion–molecule reactions, resulting in a significant class of interstellar molecules (Bohme 2009; Omont 2016; Zhen et al. 2019a, b). Furthermore, the sizes of some large fullerene/PAH clusters can fall into the range of a few nanometres, and when they are condensed, they may further combine into the cosmic dust that as part of the cosmic grains. Therefore, laboratory studies on the formation of fullerene/PAH clusters can offer a possible formation route for the grains and provide insight to understand the evolution of carbon-rich molecules (Marin et al. 2020).

Bohme (2009, 2016) studied the reactions between fullerene ions and ‘linear’ or ‘condensed’ PAHs (such as tetracene, corannulene) using a selected-ion flow tube and discussed the difference in the reaction channels. García-Hernández & Díaz-Luis (2013a), García-Hernández, Cataldo & Manchado (2013b) studied the IR spectra of C_{60} /anthracene Diels–Alder adducts by using Fourier transform IR spectroscopy, and they found that the adducts showed similar spectral features to C_{60} and other unidentified IR emission features. In addition, Dunk et al. (2013) studied the gas-phase interactions of fullerenes C_{60} and C_{70} with coronene ($C_{24}H_{12}$) under energetic conditions, and the results showed that various cluster cations were formed and exhibited covalent bond features. Since then, studies from the Zettergren et al. (2010, 2013) and Delaunay et al. (2015) groups have shown that new chemically bonded molecular species are formed by the collision between several keV atomic ions and van der Waals clusters of fullerene (C_{60}) and PAHs (e.g. pyrene, $C_{16}H_{10}$).

In the laboratory, research and reproduction of the process from simple molecules to larger gas-phase molecular clusters and eventually to dust grains is one of the most fundamental questions. Our group recently investigated the formation and photodissociation of fullerene/anthracene, fullerene/9-vinylanthracene, and fullerene/9-

methylanthracene cluster cations (Zhen et al. 2019a, b). The functionalization from aromatic H, methyl, vinyl, to other groups (here, the amino group) may change the ease of reaction, the reaction products, or the addition of multiple PAH clusters.

To characterize the growth of clusters by adding monomers (with the amino group), and to open new reaction formation routes, in this work, the reaction between cationic fullerenes and amino-substituted PAHs is studied. We select 9-amioanthracene ($C_{14}H_{11}N$, $m/z = 193$) as an example of an amino-substituted PAH. We carry out a laboratory investigation into the ion–molecule reactions between fullerene cations ($C_{60/58/56/54}^+$) and 9-amioanthracene in the gas phase. For the newly formed fullerene/9-amioanthracene clusters, quantum chemistry calculations are performed to determine their molecular structures and formation mechanisms.

2 EXPERIMENTAL RESULTS

The experiment was performed on apparatus equipped with a quadrupole ion trap and reflection time-of-flight mass spectrometer (experimental details provided in the supplementary material) (Zhen et al. 2019a, b). The obtained mass spectrum of cationic fullerene/9-amioanthracene clusters is presented in Fig. 1. Fullerene/9-amioanthracene cluster cations $(C_{14}H_{11}N)_n C_{58/56}^+$ with $n = [1, 7]$ and $(C_{14}H_{11}N)_m C_{54}^+$ with $m = [1, 5]$ are observed. No clusters involving C_{60}^+ are detected. We will discuss the formation behaviour in view of the theoretical calculation in the next section.

For the formation pathways of fullerene-fragment (C_{54} , C_{56} , and C_{58})/9-amioanthracene cluster cations, we think that the fullerene-fragment-derived cluster cations are formed by ion–molecule reaction pathways, i.e. $C_{54/56/58}^+$ cations + neutral 9-amioanthracene molecule (Bohme 2016; Zhen et al. 2019a, b). In the ion trap, fullerene/9-amioanthracene clusters are formed via collision reactions between fullerene ions and 9-amioanthracene and stabilized

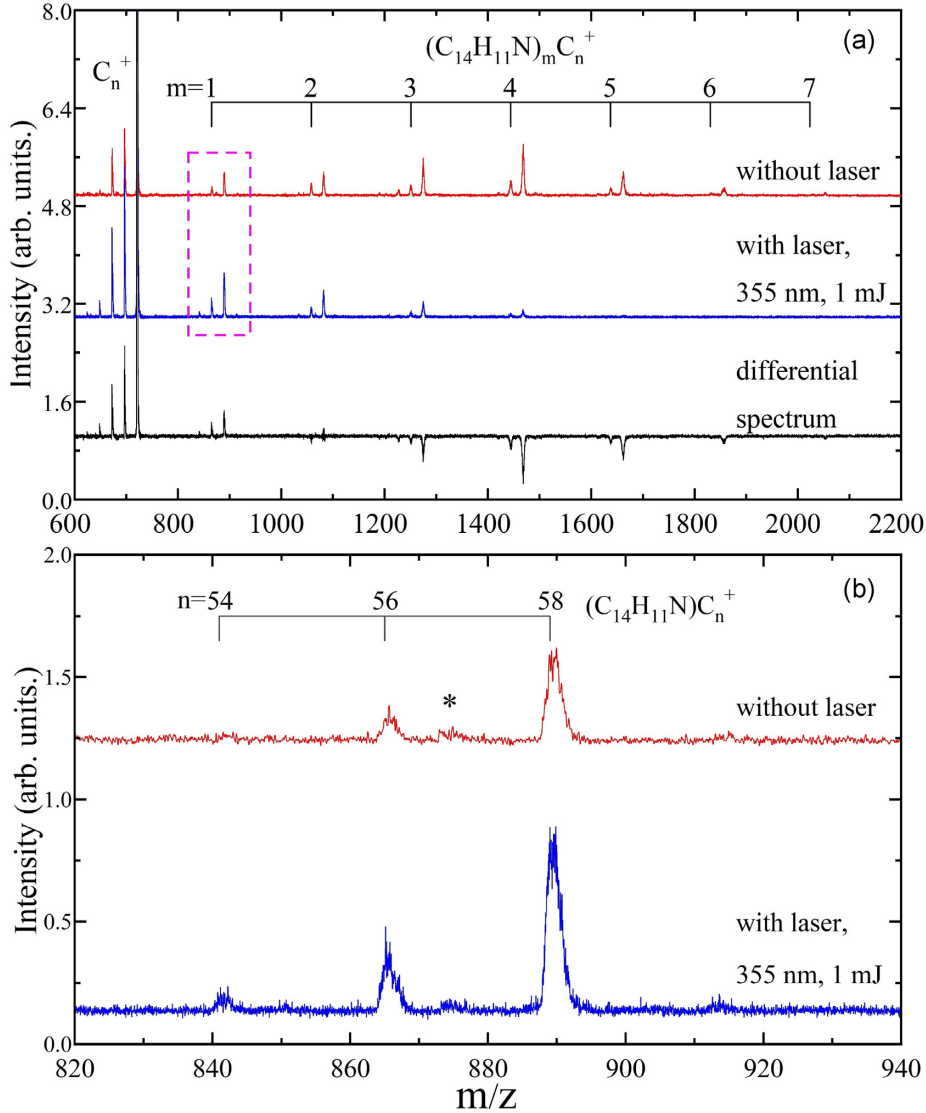
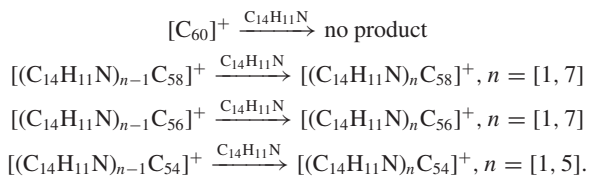


Figure 2. (a) Mass spectrum of cationic fullerene/9-aminoanthracene clusters recorded with 355 nm laser irradiation with an energy of 1.0 mJ and irradiation time 2.08 s (7.8–9.88 s) (blue trace). The mass spectrum recorded without laser irradiation is also shown in the upper red trace. The lower black trace shows the differential spectrum in laser-on and laser-off conditions; (b) an enlarged mass spectrum of cationic fullerene/9-aminoanthracene clusters recorded without laser irradiation (red trace) and with laser irradiation (blue trace) in the range of $m/z = 820\text{--}940$. The feature marked with * is $(\text{C}_{14}\text{H}_{10})\text{C}_{58}^+$, due to contaminations in the ion trap chamber.

by collision with the buffer gas helium. Clusters were probably formed by continuous reactions step by step. That is, fullerene ions first reacted with one 9-aminoanthracene molecule to form mono-9-aminoanthracene adducts, and some of the mono-9-aminoanthracene adducts then react with another 9-aminoanthracene molecule to form bis-9-aminoanthracene adducts. Other large clusters were formed in a similar way. The formation pathways for fullerene/9-aminoanthracene clusters are suggested below:

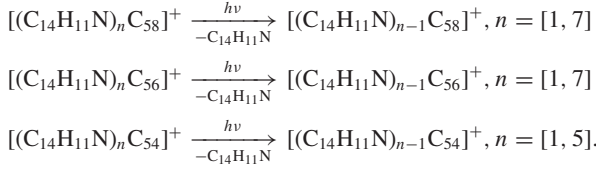


To characterize the photodissociation behaviour of cationic fullerene/9-aminoanthracene clusters, a 355 nm laser beam with an

energy of 1.0 mJ pulse⁻¹ was used to irradiate the trapped cluster cations, and the irradiation time is 2.08 s (in the range of 7.8–9.88 s). The resulting mass spectrum is shown in Fig. 2(a). The intensity of larger clusters decreases while the intensity of smaller clusters and fullerene ions increases. Further detailed comparison is clearly shown in the differential spectrum (the bottom trace in Fig. 2a). We note that the differential spectrum of the two experiments can be associated not only with the effect of laser irradiation, but also with the introduction of a time delay before the extraction of ions from the trap. In the differential spectrum, C_{60}^+ exhibits a non-zero intensity, which will be discussed in the next section.

Fig. 2(b) displays an enlarged partial mass spectra recorded with and without laser irradiation. Only photofragments with the loss of 9-aminoanthracene molecules are observed, and no other fragment channels (e.g. dehydrogenated) are observed. It indicates that fullerene/9-aminoanthracene clusters dissociate into small ones by shedding 9-aminoanthracene molecules, and there

is no dehydrogenation channel upon laser irradiation (e.g. 355 nm, 1.0 mJ pulse⁻¹). Accordingly, we propose the following photodissociation pathways for fullerene/9-aminoanthracene cluster cations:



3 THEORETICAL CALCULATION RESULTS

To better understand the formation mechanisms for cationic fullerene/9-aminoanthracene clusters, quantum chemistry calculations have been performed (theoretical details are provided in the supplementary material). For fullerene cations, 9-aminoanthracene, and their mono-9-aminoanthracene adduct, frequency calculations were also performed based on their optimized geometries. Furthermore, the zero-point energy and thermal corrections can be obtained from the frequency calculation to correct the molecular energy. However, there exists some difficulty in frequency calculation for larger molecules. Therefore, only geometry optimizations are done for larger fullerene/9-aminoanthracene clusters (containing two or more 9-aminoanthracene molecules); their energy does not include zero-point energy or thermal corrections.

The molecular geometry of C_{58}^+ is obtained by C_2 unit loss; we assume that there is no carbon skeleton rearrangement (except for the C_2 loss at a local position) during the electron impact ionization and fragmentation process (Zhen et al. 2019a; Candian et al. 2019). Fullerene cations and fullerene/9-aminoanthracene cluster cations have open-shell electronic structures, and the spin multiplicity for the ground state is assumed to be 2. The neutral fullerenes and 9-aminoanthracene have closed-shell electronic structures, and their spin multiplicity is thus set as 1.

As shown in Fig. 3, the reactants, transition states, intermediary, product, and energy for the reactions of C_{60}^+ , C_{58}^+ with 9-aminoanthracene are obtained. For the reaction of C_{60}^+ and 9-aminoanthracene, one representative combination site on C_{60}^+ is considered (Fig. 3a). For the reaction of C_{58}^+ and 9-aminoanthracene, two representative combination sites on C_{58}^+ , i.e. the 7 C-ring and the opposite 6 C-ring are taken into consideration (Figs 3b and c).

Fig. 3(a) depicts the mechanism for the reaction of C_{60}^+ + 9-aminoanthracene. Two competing reaction channels, the charge transfer channel and the adduct formation channel, are considered. The charge transfer channel is a barrier-free pathway, and the process is exothermic with 0.9 eV. To the adduct formation channel, the van der Waals molecules are first formed in the collision reaction stage. Some of the molecules can be stabilized by collision with the buffer gas, helium, while some of them can be converted into covalently bonded molecules via one (or two) transition state (or states) and intermediate states. As presented in Fig. 3(a), the van der Waals molecule initially forms with an exothermic energy of 1.5 eV. After going through two transition states (with barrier energies of 1.0 and 0.1 eV, respectively) and one intermediary, covalently bonded molecules are formed. The binding energy for covalently bonded molecules is determined as 0.9 eV, corresponding to C_{60}^+ and 9-aminoanthracene, which is smaller than that for van der Waals molecules.

Figs 3(b) and (c) show the mechanisms for the reaction between C_{58}^+ and 9-aminoanthracene. The charge transfer process is exothermic with 0.4 eV, less than the C_{60}^+ and 9-aminoanthracene system.

For 9-aminoanthracene adducting on the 7 C-ring of C_{58}^+ , as shown in Fig. 3(b), van der Waals molecules are first formed with a binding energy of -1.3 eV; they then cross two transition states (0.4 and 0.3 eV, respectively) and form covalently bonded molecules. The binding energy for covalently bonded molecules is determined as 0.9 eV, corresponding to C_{58}^+ (7 C-ring) and 9-aminoanthracene, which is smaller than that for van der Waals molecules. When 9-aminoanthracene adducts on the opposite 6 C-ring of C_{58}^+ , as shown in Fig. 3(c), it first forms van der Waals molecules with a binding energy of -1.1 eV. It takes energy of 1.0 eV to cross the transition state to form covalently bonded molecules. The binding energy for covalently bonded molecules is determined as 0.7 eV, corresponding to C_{58}^+ (6 C-ring) and 9-aminoanthracene. Considering the energy loss (such as IR emission and collision) of van der Waals molecules, a minimal amount of covalently bonded molecules can be formed and neglected in the following calculation.

In addition, we also obtained some other possible adduct reaction sites for the reaction pathways of C_{60}^+ , C_{58}^+ , and 9-aminoanthracene (together with the binding energy), which are provided in the supplementary material (Fig. S1). From the currently obtained calculation results, the formation pathway is mainly dependent on the structure of fullerene cations (reaction sites or cage structures) and the functional group's PAH properties.

In combination with the observed mass spectrum, as shown in Fig. 1, there exists a competition between the charge transfer and adduct formation processes (the latter one includes the van der Waals bonding growth model versus the covalent bonding growth model). We can conclude that the charge transfer process is in dominance for the system of C_{60}^+ and 9-aminoanthracene. For the system of C_{58}^+ and 9-aminoanthracene, adduct formation is the main process with competition between the van der Waals and covalent bonding models. Three representative isomers of $(C_{14}H_{11}N)C_{58}^+$ are obtained from the calculations, i.e. as shown in Fig. 4, 9-aminoanthracene 'landing on' C_{58}^+ (7 C-ring) with a van der Waals bond $(C_{14}H_{11}N)C_{58}^+$ (P_1) and a covalent bond $(C_{14}H_{11}N)C_{58}^+$ (P_3), as well as 9-aminoanthracene 'landing on' C_{58}^+ (6 C-ring) with a van der Waals bond $(C_{14}H_{11}N)C_{58}^+$ (P_2).

Furthermore, in order to better demonstrate the binding characteristics of these newly formed molecular clusters, three-dimensional images of the highest occupied molecular orbital (HOMO) and lowest unoccupied molecular orbital (LUMO) of the van der Waals molecule and the covalently bonded molecule, as presented in Fig. 3, are obtained and provided in the supplementary material (Fig. S2).

To elucidate the formation mechanism for larger fullerene/9-aminoanthracene cluster cations, the formation routes for larger $C_{58}/9$ -aminoanthracene clusters were also investigated. Fig. 4 displays the reaction routes for the formation of $(C_{14}H_{11}N)_2C_{58}^+$. As mentioned above, three isomers (P_1 , P_2 , and P_3 in Fig. 4) of $(C_{14}H_{11}N)C_{58}^+$ are considered. When 9-aminoanthracene connects with isomers P_1 and P_3 , 9-aminoanthracene can 'land on' the 6 C-ring of C_{58}^+ . Based on the calculation results for the reaction of C_{58}^+ (6 C-ring) + $C_{14}H_{11}N$, $C_{14}H_{11}N$ possibly connects with isomers P_1 and P_3 of $(C_{14}H_{11}N)C_{58}^+$ via van der Waals bonds to form bis-9-aminoanthracene adducts $(C_{14}H_{11}N)_2C_{58}^+$ (P_1 and P_2) (P_1 is a van der Waals molecule and P_2 is a mixture of van der Waals and covalent bonds). The binding energies for the formation of adducts $(C_{14}H_{11}N)_2C_{58}^+$ (P_1 and P_2) are -0.9 eV and -1.2 eV, respectively. The 'rich' energy impels a conversion between adducts $(C_{14}H_{11}N)_2C_{58}^+$ (P_1 and P_2 , with an energy difference of 0.1 eV), i.e. converting the binding route on the 7 C-ring of C_{58}^+ between van der Waals and covalent bonds. When a 9-aminoanthracene molecule connects with isomers P_2 of $(C_{14}H_{11}N)C_{58}^+$, 9-aminoanthracene is more likely to 'land on' the active unoccupied 7 C-ring of C_{58}^+ to first

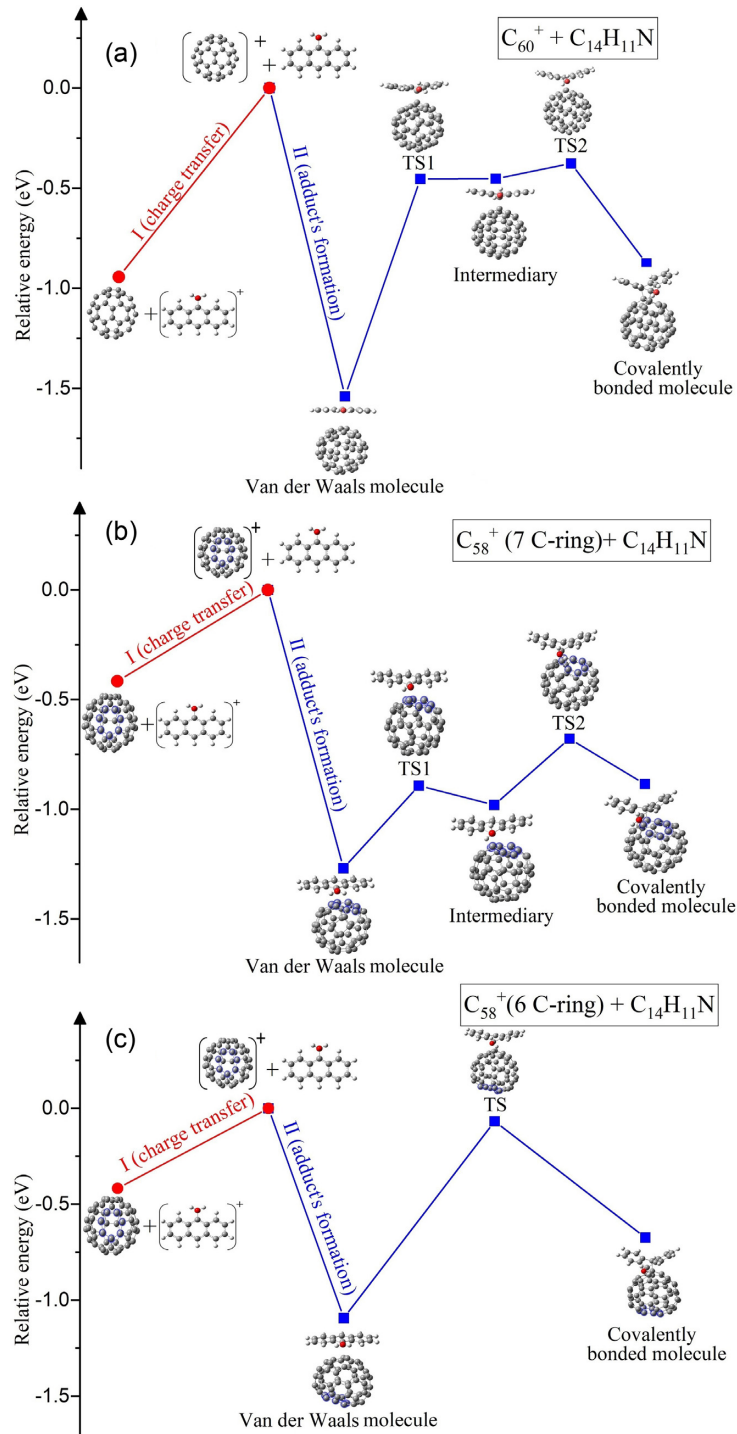


Figure 3. The reactants, transition states, intermediary, products, and their corresponding energy for the reaction pathways of C_{60}^+ , C_{58}^+ with 9-aminoanthracene: the upper panel (a) is the mechanism for the reactions of C_{60}^+ with 9-aminoanthracene; the lower panels (b) and (c) are the mechanisms for the reactions of C_{58}^+ (7 C-ring) and C_{58}^+ (6 C-ring) with 9-aminoanthracene, respectively.

form van der Waals molecules with a binding energy of -1.1 eV. The rich energy may impel a conversion on the 7 C-ring of C_{58}^+ between van der Waals and covalent bonds; i.e. there exists a conversion between adducts $(C_{14}H_{11}N)_2C_{58}^+$ (P_1 and P_2).

Fig. 5 displays the reaction routes for the formation of $(C_{14}H_{11}N)_3C_{58}^+$, $(C_{14}H_{11}N)_4C_{58}^+$, and $(C_{14}H_{11}N)_5C_{58}^+$, respectively. In panel (a), the geometry P_1 and P_2 of $(C_{14}H_{11}N)_2C_{58}^+$ are considered.

When 9-aminoanthracene connects with geometry P_1 and P_2 of bis-9-aminoanthracene adducts, 9-aminoanthracene can only ‘land’ on the unoccupied 6 C-ring of C_{58}^+ to first form tri-9-aminoanthracene adducts $(C_{14}H_{11}N)_3C_{58}^+$ (P_1 and P_2) with binding energies of -1.0 eV and -1.1 eV, respectively. This energy can induce the geometry conversation of tri-9-aminoanthracene adducts between a van der Waals molecule ($(C_{14}H_{11}N)_3C_{58}^+$, P_1) and a mixture of van der Waals

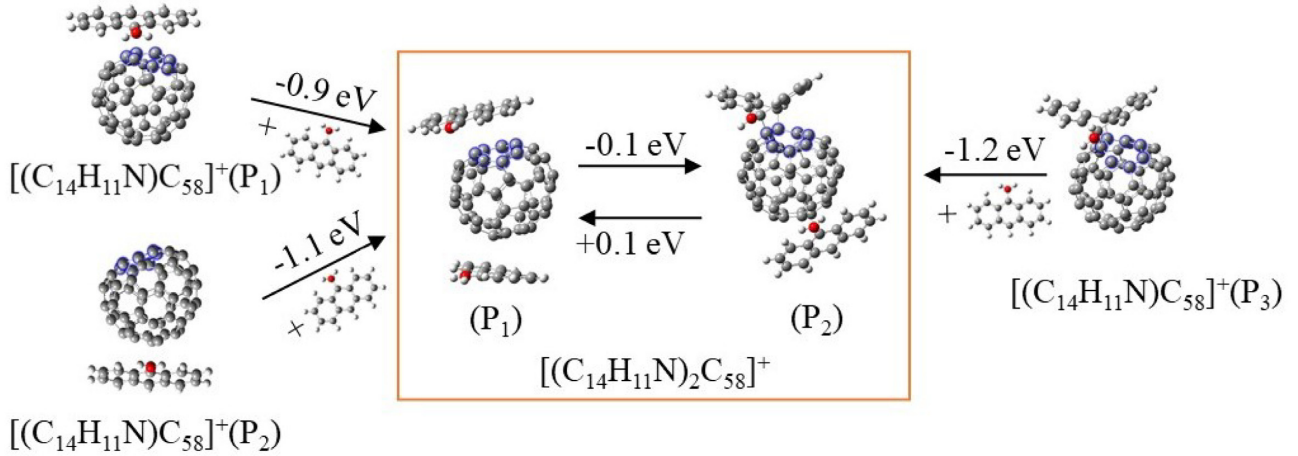


Figure 4. The formation pathways for $[(C_{14}H_{11}N)_2C_{58}]^+$.

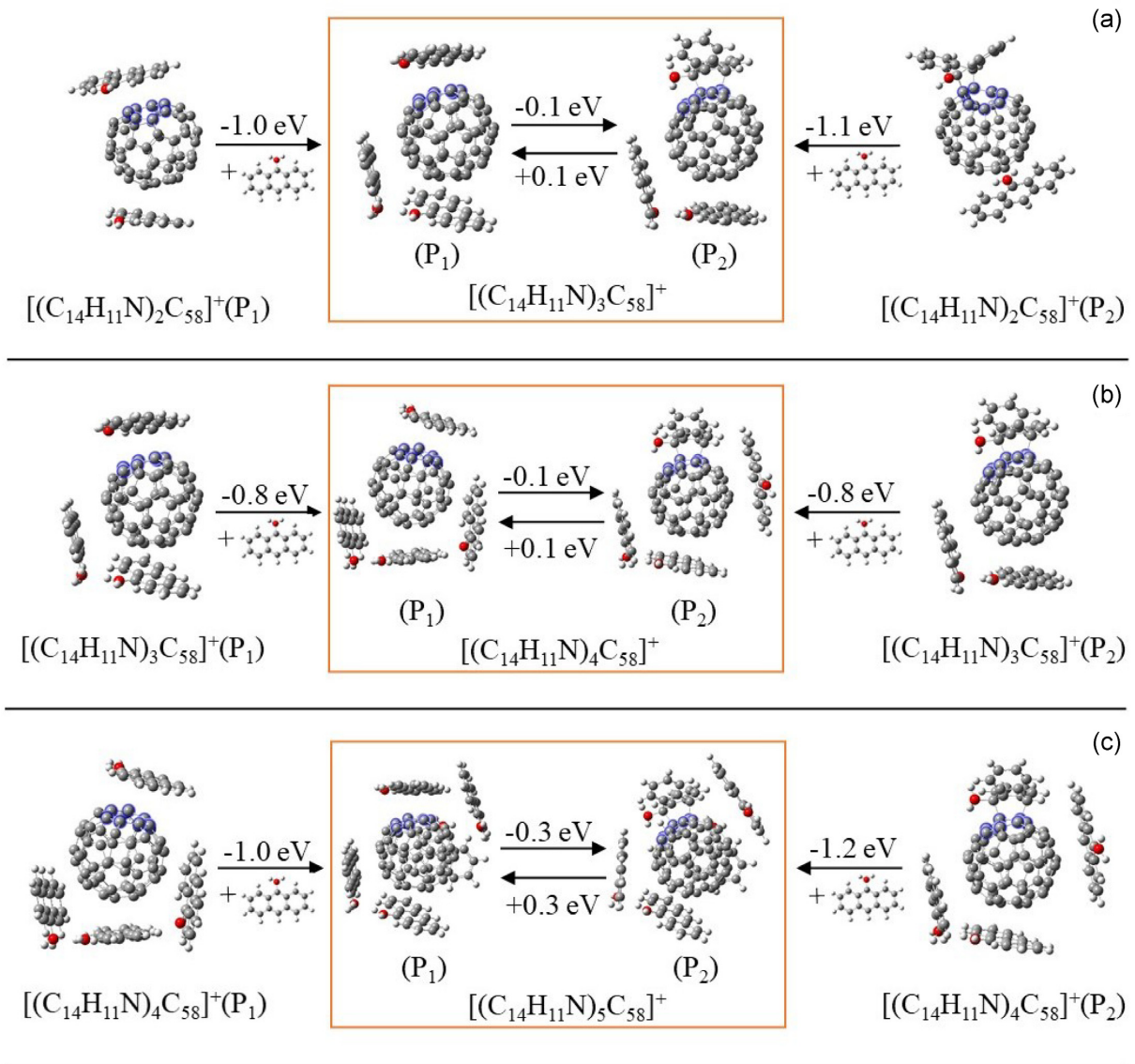


Figure 5. The formation pathways for (a) $[(C_{14}H_{11}N)_3C_{58}]^+$, (b) $[(C_{14}H_{11}N)_4C_{58}]^+$, and (c) $[(C_{14}H_{11}N)_5C_{58}]^+$, respectively.

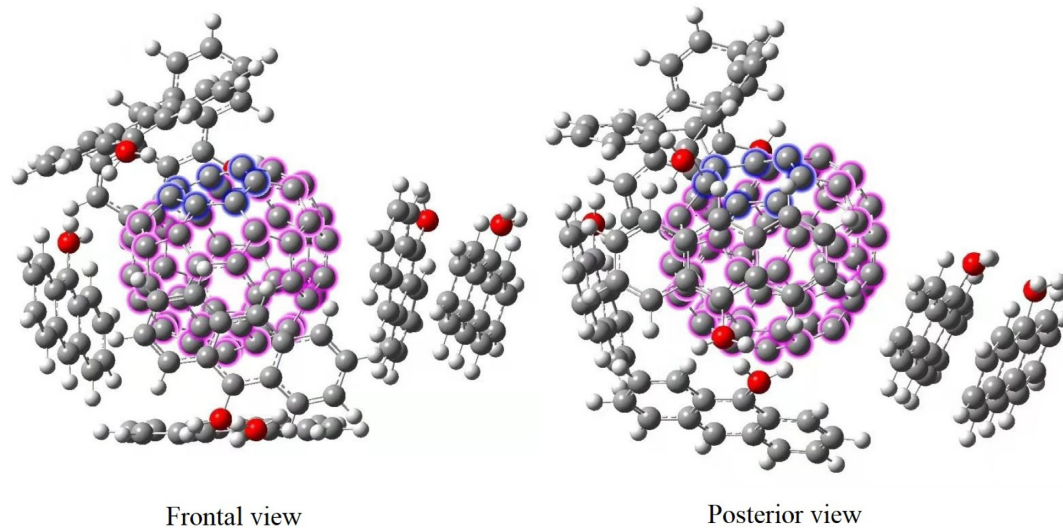


Figure 6. Theoretical optimization of one possible geometry of $(\text{C}_{14}\text{H}_{11}\text{N})_7\text{C}_{58}^+$ with frontal and posterior views.

and covalent bonds ($(\text{C}_{14}\text{H}_{11}\text{N})_3\text{C}_{58}^+$, P_2) with an energy difference of 0.1 eV. In the same way, in panels (b) and (c), the formation pathways of fullerene/9-aminoanthracene adducts $(\text{C}_{14}\text{H}_{11}\text{N})_4\text{C}_{58}^+$ and $(\text{C}_{14}\text{H}_{11}\text{N})_5\text{C}_{58}^+$ are presented and the binding energy is also ~ 1 eV. Similar to $(\text{C}_{14}\text{H}_{11}\text{N})_3\text{C}_{58}^+$, the geometry configuration conversion clearly also exists.

Due to the space steric effect, all 9-aminoanthracene molecules are evenly distributed on the surface of the sphere cage. Moreover, there is no large variation in the binding energy (all around -1.0 eV) in the process of adding 9-aminoanthracene to the cage surface. In other words, all the polymerizations should have a similar reaction pathway; the number of 9-aminoanthracene molecules attached to the surface of fullerene is mainly determined by steric effects.

The calculated binding energy is around -1.0 eV, which suggests that these fullerene/9-aminoanthracene clusters are easily destroyed. In agreement with the experimental results, with laser irradiation, they go back to fullerene ions and 9-aminoanthracene, and no H-loss fragments are involved. The photofragmentation behaviour of the fullerene/9-aminoanthracene cluster system is similar to the fullerene/PAH cluster system (Zhen et al. 2019a, b).

Fullerene/9-aminoanthracene adducts including seven 9-aminoanthracene molecules have been formed in the present experiment. Following the calculations for C_{58} /9-aminoanthracene adducts, one possible geometry of $(\text{C}_{14}\text{H}_{11}\text{N})_7\text{C}_{58}^+$ is theoretically optimized, as shown in Fig. 6. The calculation results show that it is feasible and possible for C_{58}^+ to connect with six 9-aminoanthracene molecules surrounding the first shell of C_{58}^+ (one is covalently bonded, and other five are van der Waals bonded with a fullerene cage), but it becomes difficult to add the seventh 9-aminoanthracene molecule to the first shell; based on this, the seventh 9-aminoanthracene molecule is thus added to the second shell of C_{58}^+ (van der Waals bonded with 9-aminoanthracene), resulting in a three-layer two-shells molecular cluster. The nucleus-to-nucleus diameter of this cluster measures around 4 nm.

Overall, the theoretical calculation results are consistent with the experimental results. We can conclude that ion–molecule reactions between fullerene cations and 9-aminoanthracene readily occur, resulting in a very large number of reaction pathways and very complex molecular clusters. The van der Waals bonded molecule and covalently bonded molecule are formed with an exothermic energy

around of 1.0 eV. The exothermic energy is relatively higher than the energy that can stabilize whole clusters, so we propose that fullerene/9-aminoanthracene clusters formed in the laboratory are mixed clusters with all different possible isomers. We note that we did not see the very strongly covalently bonded molecule that formed from our current theoretical calculation. Perhaps, in the formation process, possible dynamical processes play an important role; further studies will be required to address this issue.

4 DISCUSSIONS AND ASTRONOMICAL IMPLICATIONS

The experimental results show that no adducts of C_{60}^+ and 9-aminoanthracene are formed. In combination with quantum chemistry calculations, we suggest that the charge transfer process is the main channel in the collision between C_{60}^+ and 9-aminoanthracene. C_{60}^+ will go through the charge transfer channel and form more neutral C_{60} , which will limit C_{60}^+ to existing as molecular clusters. In the modelling of the intensity ratio between C_{60} and C_{60}^+ in the ISM, the conversion between the cationic and neutral states of C_{60} via the charge transfer process should be taken into consideration (Cami et al. 2010; Bernard-Salas et al. 2012; Campbell et al. 2015; Cordiner et al. 2017).

The experimental results show that smaller fullerene-fragment cations $\text{C}_{58/56/54}^+$ can interact with 9-aminoanthracene to form fullerene/9-aminoanthracene cluster cations efficiently, and the charge transfer channel is the non-primary process. The experimental results show that fullerene ions can adduct with up to seven 9-aminoanthracene molecules to form large clusters (e.g. $(\text{C}_{14}\text{H}_{11}\text{N})_7\text{C}_{58}^+$), while fullerene ions can only connect three or four anthracene, 9-vinylanthracene, or 9-methylanthracene molecules in similar experimental conditions (we assume that the small differences between these experimental conditions will not change the chemical reaction pathway, and PAH species are always in excess when compared to the number of fullerene cations trapped in the ion trap). The reason for the difference in the cluster sizes is the influence of the amino group ($-\text{NH}_2$) in 9-aminoanthracene (Zhen et al. 2019a, b).

The mechanisms for the reaction of C_{58}^+ and 9-aminoanthracene have been investigated by theoretical calculations. For the fullerene/anthracene, fullerene/9-methylanthracene, and fullerene/9-

vinylanthracene systems, the covalently bonded clusters are favourable because of their higher stability with respect to the van der Waals bonded clusters (Zhen et al. 2019a, b). However, the bonding features are very different in the fullerene (C_{58}^+)/9-aminoanthracene system. Their van der Waals bonded clusters are more stable than the covalently bonded clusters. Considering the barrier involved between these two clusters, the calculations show that when 9-aminoanthracene ‘lands on’ the 6 C-ring of C_{58}^+ , they probably connect via van der Waals forces; when 9-aminoanthracene ‘lands on’ the 7 C-ring of C_{58}^+ , they may connect via van der Waals or covalent bonds. More importantly, due to the special binding feature on the 7 C-ring of C_{58}^+ , there exists structural conversion between van der Waals molecules and mixtures of van der Waals and covalent bonds for C_{58}^+ /9-aminoanthracene cluster cations. The cluster formation pathways through ion–molecular collision reactions presented here offer a probable approach to carbonaceous grains in space and provide an insight into their constitution and structural properties (Tielens 2008; Galliano, Galametz & Jones 2018).

The calculated exothermic energy for each step of C_{58}^+ /9-aminoanthracene clusters is around 1.0 eV, and the exothermic energy does not have a large variation in the process of adding all of the 9-aminoanthracenes. The exothermic energy can quickly be transferred as the vibrational energy of ground states to ‘heat’ the clusters, resulting in a temperature increase (ΔT). The temperature rise can be estimated precisely for small molecules based on the result of frequency calculations: $(C_{14}H_{11}N)C_{58}^+$ (P_1), $\Delta T = 374$ K; $(C_{14}H_{11}N)C_{58}^+$ (P_2), $\Delta T = 352$ K; $(C_{14}H_{11}N)C_{58}^+$ (P_3), $\Delta T = 324$ K, respectively. Using an expression for the PAH system (Tielens 2005), we can roughly estimate the temperature increase for the C_{58}^+ /9-aminoanthracene cluster system: $\Delta E = 1.0$ eV; N is the atom number of clusters, ΔN is the atom number of adducts; here, $\Delta N = 26$ ($C_{14}H_{11}N$, $14+11+1 = 26$):

$$\Delta T \approx 2000 \left(\frac{\Delta E}{N + \Delta N} \right)^{0.4}.$$

$\Delta T = 340$ K is derived for C_{58}^+ on addition of the first 9-aminoanthracene, while $\Delta T = 223$ K is derived for $(C_{14}H_{11}N)_6C_{58}^+$ on the addition of one 9-aminoanthracene. From the calculation results, the increased temperature falls very quickly when the C_{58}^+ /9-aminoanthracene clusters become larger. This indicates that larger C_{58}^+ /9-aminoanthracene clusters are more stable to the impact of whole-system energy variation.

In our experimental conditions, we suppose that the exothermic energy is mainly released through collision with He atoms (buffer gas); IR fluorescence may not play an important role in exothermic energy release processes. In contrast to our laboratory studies, in astrophysical environments, due to the very low density of molecules, the exothermic energy is mainly released through IR fluorescence. However, irrespective of which energy release pathways are involved, it will always leave the species at a lower level of vibrational excitation from which it relaxes either through collision relaxation or IR fluorescence. In the present study, we will assume that this is the case to the end and, hence, we directly apply our experimental results to the formation processing of large molecular clusters or interstellar dust in space.

The largest fullerene/9-aminoanthracene cluster, $(C_{14}H_{11}N)_7C_{58}^+$, which contains 240 atoms, has a nucleus-to-nucleus diameter of around 4 nm. The size of these fullerene/PAH-derived clusters approaches that of very small grains. If we set aside the limitations of our experimental conditions, we can make a relatively reasonable guess that such molecular clusters can continue to grow at their

current size (adduct on the third layer of this clusters); i.e. in a favourable environment of interstellar space, it may be possible to eventually form molecular clusters with sizes of the order of micrometres through the ways mentioned above (Jäger et al. 2009; Berné, Montillaud & Joblin 2015).

Since PAHs, C_{60} , and C_{60}^+ have been confirmed in the interstellar medium, we expect that their fullerene/PAH derived clusters (i.e. fullerene/PAH clusters) might also coexist in space. However, the spatial distributions of fullerenes and smaller PAHs do not overlap in planetary nebulae; we do not propose fullerene/PAH adducts as such contributors. In particular, in the harsh interstellar environment, small PAHs and their derivatives, such as 9-aminoanthracene molecules, hardly survive (Tielens 2008). Nevertheless, species formed by reactions between fullerene cations and molecules found in planetary nebulae may be involved. The coexisting molecules, not only specific PAHs, containing functional groups, especially the amino group ($-NH_2$), may be involved in dust particle growth. From our current study, we can conclude that nitrogen matters (e.g. $-NH_2$)! The specific side chains play a more important role in the cluster or dust formation process. The mechanisms for the reaction of fullerene ions and 9-aminoanthracene presented here, which can be treated as an indicator for understanding the interstellar carbonaceous dust growth mechanism, help us understand the interactions between interstellar fullerene ions and amino-bearing PAHs. These two interstellar species may form clusters with multishelled structural features, and then this structure can connect with multi-amino-bearing PAHs to form large clusters (Rapacioli et al. 2006; Candian et al. 2018).

In addition, these fullerene/9-aminoanthracene clusters may also provide candidates of interest for the IR interstellar bands (Tielens 2013). Because the structure of fullerene/9-aminoanthracene clusters initially formed is diverse, their role in the spectral profile contribution and spectral features for tentative detections in the ISM is warranted. For example, for $(C_{14}H_{11}N)C_{58}^+$, the IR spectral features of the three isomers that may be formed (as shown in Fig. 3, 9-aminoanthracene ‘landing on’ C_{58}^+ (7 C-ring) with a van der Waals bond $(C_{14}H_{11}N)C_{58}^+$ (P_1) and covalent bond $(C_{14}H_{11}N)C_{58}^+$ (P_3), as well as 9-aminoanthracene ‘landing on’ C_{58}^+ (6 C-ring) with a van der Waals bond $(C_{14}H_{11}N)C_{58}^+$ (P_2)) should be relatively different. Further observational and theoretical studies are required to address this issue.

5 CONCLUSIONS

In conclusion, we have obtained experimental and theoretical results on the formation and photoevolution processes of cationic fullerene/9-aminoanthracene clusters. The growth mechanisms of clusters by adding PAH monomers, here with the amino group, open up new reaction formation routes. These results demonstrate the importance of molecule–ion reactions in synthesizing large fullerene/PAH derivatives in a bottom-up process, and provide an insight into the charge transfer model competition with the van der Waals growth bonding mode and the covalent growth bonding mode in the formation process of larger gas-phase molecular clusters in the ISM. Also, from our current study, nitrogen matters! The specific side chains, e.g. the amino group ($-NH_2$), can play an important role in the interstellar dust growth process in the ISM.

ACKNOWLEDGEMENTS

This work is supported by the Strategic Priority Research Program of the Chinese Academy of Sciences, Grant No. XDB 41000000, and from the National Natural Science Foundation of China (NSFC,

Grant No. 12073027 and Grant No. 41625013). YC acknowledges the grant from the National Natural Science Foundation of China (NSFC, Grant No. 21827804). Theoretical calculations were performed at the Supercomputing Center of the University of Science and Technology of China.

DATA AVAILABILITY

All data generated or analysed during this study are included in this article.

REFERENCES

- Allamandola L. J., Tielens A. G. G. M., Barker J. R., 1989, *ApJS*, 71, 733
 Bernard-Salas J., Cami J., Peeters E., Jones A. P., Micelotta E. R., Groenewegen M. A. T., 2012, *ApJ*, 757, 41
 Berné O., Tielens A. G. G. M., 2012, *Proc. Natl. Acad. Sci.*, 109, 401
 Berné O., Montillaud J., Joblin C., 2015, *A&A*, 577, A133
 Bohme D. K., 2009, *Mass Spectrometry Rev.*, 28, 672
 Bohme D. K., 2016, *Philos. Trans. A Math. Phys. Eng. Sci.*, 374, 20150321
 Cami J., Bernard-Salas J., Peeters E., Malek S. E., 2010, *Science*, 329, 1180
 Campbell E. K., Holz M., Gerlich D., Maier J. P., 2015, *Nature*, 523, 322
 Candian A., Zhen J., Tielens A. G. G. M., 2018, *Phys. Today*, 71, 38
 Candian A., Rachid M. G., MacIsaac H., Staroverov V. N., Peeters E., Cami J., 2019, *MNRAS*, 485, 1137
 Cordiner M. A. et al., 2017, *ApJ*, 843, L2
 Cordiner M. A. et al., 2019, *ApJ*, 875, L28
 Delaunay R. et al., 2015, *J. Phys. Chemistry Lett.*, 6, 1536
 Dunk P. W., Adjizian J. J., Kaiser N. K., Quinn J. P., Blakney G. T., Ewels C. P., Marshall A. G., Kroto H. W., 2013, *Proc. Natl. Acad. Sci.*, 110, 18081
 Galliano F., Galametz M., Jones A. P., 2018, *ARA&A*, 56, 673
 García-Hernández D. A., Díaz-Luis J. J., 2013a, *A&A*, 550, L6
 García-Hernández D. A., Cataldo F., Manchado A., 2013b, *MNRAS*, 434, 415
 Jäger C., Huisken F., Mutschke H., Llamas Jansa I., Henning T., 2009, *ApJ*, 696, 706
 Marin L. G., Bejaoui S., Haggmark M., Svadlenak N., de Vries M., Sciamma-O'Brien E., Salama F., 2020, *ApJ*, 889, 101
 Martínez L. et al., 2020, *Nat. Astron.*, 4, 97
 Omont A., 2016, *A&A*, 590, A52
 Rapacioli M., Calvo F., Joblin C., Parneix P., Toubanc D., Spiegelman F., 2006, *A&A*, 460, 519
 Sellgren K., 1984, *ApJ*, 277, 623
 Tielens A. G. G. M., 2005, *The Physics and Chemistry of the Interstellar Medium*, 1st edn. Cambridge Univ. Press, Cambridge
 Tielens A. G. G. M., 2008, *ARA&A*, 46, 289
 Tielens A. G. G. M., 2013, *Rev. Modern Phys.*, 85, 1021
 Walker G. A. H., Bohlender D. A., Maier J. P., Campbell E. K., 2015, *ApJ*, 812, L8
 Zettergren H. et al., 2010, *J. Chemical Phys.*, 133, 104301
 Zettergren H. et al., 2013, *Phys. Rev. Lett.*, 110, 185501
 Zhen J., Castellanos P., Paardekooper D. M., Linnartz H., Tielens A. G. G. M., 2014, *ApJ*, 797, L30
 Zhen J., Chen T., Tielens A. G. G. M., 2018, *ApJ*, 863, 128
 Zhen J., Zhang W., Yang Y., Zhu Q., Tielens A. G. G. M., 2019a, *ApJ*, 887, 70
 Zhen J., Zhang W., Yang Y., Zhu Q., 2019b, *MNRAS*, 490, 3498

SUPPORTING INFORMATION

Supplementary data are available at *MNRAS* online.

Figure S1. The theoretical calculation results of some other possible adduct reaction sites for the reaction pathways of C_{60}^+ , C_{58}^+ , and 9-aminoanthracene.

Figure S2. The theoretical calculation results of 3D images of the HOMO and LUMO of the van der Waals molecule and the covalently bonded molecule obtained in Fig. 3.

Please note: Oxford University Press is not responsible for the content or functionality of any supporting materials supplied by the authors. Any queries (other than missing material) should be directed to the corresponding author for the article.

This paper has been typeset from a $\text{\TeX}/\text{\LaTeX}$ file prepared by the author.